Insight into the measurement of dissolved 227Ac in seawater using radium delayed coincidence counter

Emilie Le Roy, Virginie Sanial, Francois Lacan, Pieter van Beek, Marc Souhaut, Matthew A Charette, Paul Henderson

Le Roy, E., Sanial, V., Lacan, F., van Beek, P., Souhaut, M., Charette, M. A. and Henderson, P. B.: Insight into the measurement of dissolved 227Ac in seawater using radium delayed coincidence counter, Marine Chemistry, doi:10.1016/j.marchem.2019.04.002, 2019.

Insight into the measurement of dissolved ^{227}Ac in seawater using radium delayed coincidence counter

Emilie Le Roy[a,*], Virginie Sanial[b], Francois Lacan[a], Pieter van Beek[a], Marc Souhaut[a], Matthew A. Charette[c], Paul B. Henderson[c]

[a] *LEGOS, Laboratoire d'Etudes en Géophysique et Océanographie Spatiales (Université de Toulouse, CNRS/CNES/IRD/UPS), Observatoire Midi Pyrénées, 14 Avenue Edouard Belin, 31400 Toulouse, France*
[b] *Division of Marine Science, University of Southern Mississippi, Stennis Space Center, MS 39529, USA*
[c] *Department of Marine Chemistry and Geochemistry, Woods Hole Oceanographic Institution, Woods Hole, MA 02543, USA*

A B S T R A C T

Due to the low abundance of ^{227}Ac in seawater, the analysis of this radionuclide requires the use of high-sensitivity, low-background instruments and the collection of large volume samples. A promising technique relies on the pre-concentration of ^{227}Ac in seawater using cartridges impregnated with manganese oxide (Mn-cartridges) that are mounted on in situ pumps, and its measurement on a Radium Delayed Coincidence Counter (RaDeCC), usually used to analyze short-lived radium isotopes. In this work, we present an evaluation of this technique, including 1) the study of the performance of the RaDeCC measurements for ^{227}Ac fixed on Mn-cartridges (backgrounds, detector efficiency, repeatability), and 2) the determination of the efficiency of seawater ^{227}Ac extraction of the Mn-cartridges and its reproducibility for the first time, by using Mn-cartridges placed in series. Overall, we found a Mn-cartridge extraction efficiency of 47 ± 12% (1 SD). Repeatability experiments allowed us to estimate the uncertainties of the entire measurement of 19% (1 SD). Finally, in the aim to validate the method, the ^{227}Ac activities thus obtained are compared 1) to the ^{227}Ac activities determined in several samples using Mn-fibers (assuming 100% yield of ^{227}Ac extraction) and 2) to the ^{231}Pa activities determined at the same stations during the GEOVIDE cruise (GEOTRACES GA01), ^{231}Pa being the parent nuclide of ^{227}Ac (Deng et al., 2018). Only few studies ^{227}Ac and ^{231}Pa have been published so far due to the difficulty to analyze these two nuclides. First, the ^{227}Ac activities determined using Mn-cartridges agree well with the ^{227}Ac activities determined using Mn-fibers. Second, at depths where ^{227}Ac is usually found to be in secular equilibrium with ^{231}Pa (0–2000 m), we found good agreement between ^{227}Ac and ^{231}Pa, which validates the method used to determine ^{227}Ac activities, including the estimate of the Mn-cartridge extraction efficiency.

1. Introduction

Actinium-227 (^{227}Ac; $T_{1/2}$ = 21.8 y) is produced by the radioactive decay of its parent isotope protactinium-231 (^{231}Pa; $T_{1/2}$ = 32,760 y), itself produced by the decay of uranium-235 (^{235}U; $T_{1/2}$ = 7.04 10^8 y). Oceanic ^{235}U concentrations are mostly constant through space and time due to a long residence time (~0.5 Ma; Ku et al., 1977), which leads to a uniform production rate of ^{231}Pa. Once produced, ^{231}Pa is adsorbed onto particles, and is transported to the seafloor, where it accumulates in deep-sea sediments (Anderson et al., 1983). The decay of ^{231}Pa to ^{227}Ac in the sediments is followed by partial release of ^{227}Ac due to its higher solubility (Anderson et al., 1983; Nozaki, 1993, 1984) thus leading to an ^{227}Ac flux to the overlying water column (Nozaki, 1993, 1984; Nozaki et al., 1990). Being mostly soluble, ^{227}Ac is redistributed in the ocean through water mass transport and mixing. Assuming steady state, ^{227}Ac produced in the water column is expected to be in secular equilibrium with ^{231}Pa. ^{227}Ac that diffuses out of deep-sea sediments leads to the observation of excess ^{227}Ac activities ($^{227}Ac_{ex}$) in deep waters, usually below 2000 m (Geibert et al., 2002; Nozaki, 1984; Nozaki et al., 1990). Hydrothermal vents have also been identified as an additional source of ^{227}Ac to the deep ocean (Kipp et al., 2015). Due to its deep-sea source, ^{227}Ac has been used to quantify vertical mixing and as a tracer of deep ocean circulation at basin scales and/or timescales of ca. 100 y (Geibert et al., 2002; Koch-Larrouy et al., 2015; Nozaki, 1984). Because vertical advection can also bring ^{227}Ac towards the sea surface, ^{227}Ac has also been used to estimate upwelling rates (Geibert et al., 2002).

^{227}Ac concentrations are especially low within the ocean, the total oceanic inventory being only 37 mol or 8.4 kg (Geibert et al., 2008). As a result, relatively few studies have been reported to date (Dulaiova et al., 2012; Geibert et al., 2008, 2002; Geibert and Vöge, 2008; Kipp et al., 2015; Koch-Larrouy et al., 2015; Nozaki, 1993, 1984; Nozaki et al., 1998, 1990; Shaw and Moore, 2002). The analysis of ^{227}Ac thus requires handling large volumes (typically > 200 L), from which ^{227}Ac is extracted, either through Fe or Mn hydroxide coprecipitation (Geibert and Vöge, 2008) or through sorption onto media impregnated with

MnO_2 (Shaw and Moore, 2002). Shaw and Moore (2002) reported a method for the analysis of ^{227}Ac in seawater based on the extraction of ^{227}Ac from seawater on acrylic fibers impregnated with manganese oxide (Mn-fibers), followed by its analysis using a Radium Delayed Coincidence Counter (RaDeCC; Moore and Arnold, 1996). However, passing hundreds of liters of seawater through Mn-fibers is not easy is time consuming and prevents from building vertical profiles of ^{227}Ac with a high resolution. To reduce the sample volume requirement, ^{227}Ac can be determined using alpha spectrometry that requires only 20-80 L of seawater at typical ocean activities (Geibert and Vöge, 2008). However, this approach requires lengthy steps of chemical purification and separation of ^{227}Ac prior to analysis.

Alternatively, ^{227}Ac can be extracted from large volumes of seawater using Mn-cartridges mounted on in situ pumping systems (Henderson et al., 2013). This allows for extraction of ^{227}Ac from seawater at depth without having to bring the water onboard for extraction onto Mn fibers. In this work, we evaluate the performance of this extraction method that is followed by the use of RaDeCC to quantify ^{227}Ac activities. Samples used herein were collected along the GEOVIDE section in the North Atlantic (GEOTRACES GA01). We discuss the limit of quantification and the uncertainties associated with the ^{227}Ac activities determined using RaDeCC. The repeatability (see Joint Committee for Guides in Metrology (2008) for metrology vocabulary definitions) is assessed by repeated analysis. We quantify the yield of ^{227}Ac extraction onto the Mn-cartridges using two Mn-cartridges mounted in series. The ^{227}Ac activities thus obtained can be compared with the ^{227}Ac activities determined in several samples using Mn-fibers (following Shaw and Moore, 2002). Finally, in the aim to further validate the method, we report two seawater ^{227}Ac vertical profiles in the North Atlantic Ocean and compare them to the vertical profiles of ^{231}Pa activity from the same stations and with historical data. Above 2000 m, where ^{227}Ac is expected to be in secular equilibrium with ^{231}Pa, such a comparison provides independent validation and assesses the trueness (see Joint Committee for Guides in Metrology, 2008 for metrology vocabulary definitions) of the procedure as a whole.

2. Materials and methods

2.1. Sample collection

The samples were collected in the framework of the GEOVIDE section (GEOTRACES GA01; PIs: Géraldine Sarthou, LEMAR, France and Pascale Lherminier, LOPS, France) that was conducted in the North Atlantic Ocean between Lisbon, Portugal and St John's, Canada (15 May - 30 June 2014). Along the section, nine stations were sampled for ^{227}Ac. ^{227}Ac was extracted from seawater using two Mn-cartridges placed in series on in situ pumps. As a comparison, several discrete, large volume samples were also collected using Niskin bottles, and passed by gravity through Mn-fibers. Here, we report on the validation of the method used to determine dissolved ^{227}Ac activities. The ^{227}Ac activities determined for the entire GEOVIDE section will be shown in a separate paper.

2.1.1. Sample preparation and extraction of ^{227}Ac using Mn-cartridges

Several cartridges designed to be mounted on in situ pumps were prepared using a protocol slightly modified from Henderson et al. (2013). Acrylic fiber cartridges of 25.4 cm (10 in.) long with 5 µm porosity were cut to obtain a final size of 77 mm ± 0.4 mm, which is slightly smaller than the cartridges prepared by Henderson et al. (2013). The cartridges were soaked in a milli-Q water bath for 48 h. The cartridges were then impregnated with MnO_2 by soaking in a saturated $KMnO_4$ bath at room temperature for 48 h. In addition, circulation of a saturated $KMnO_4$ solution through the cartridges served to improve the MnO_2 impregnation within the cartridge itself with the aim of increasing the cartridge extraction efficiencies for ^{227}Ac (and other radionuclides). Mn-cartridges were rinsed after the final step with radium-free milli-Q water and then vacuum packed in a sachet.

At each station, large volume in situ pumps (ISP) (Challenger and McLane) were deployed at 6 to 13 depths for 3 to 4 h, which resulted in filtration volumes of 418 to 1565 L at flow rates of 3-6 L min^{-1}. Seawater first passed through Supor (Pall, 0.8 µm pore size) or QMA (Sartorius, 1 µm pore size) membranes (to collect suspended particles), then through the Mn-cartridges to preconcentrate ^{227}Ac. For the deep samples, two Mn-cartridges (A Mn-cartridge and B Mn-cartridge) were placed in series in order to provide information on the yield of ^{227}Ac fixation (see section 3.2.). For shallow samples, single cartridges were mounted on the in-situ pumps. Following collection, each Mn-cartridge was rinsed with Ra-free milli-Q water and slightly dried using compressed air. Similar to Mn-fibers (Sun and Torgersen, 1998), the moisture of the Mn-cartridges may affect the emanation efficiency of radon that is actually the radionuclide quantified using the RaDeCC systems (see 2.2). According to Sun and Torgersen (1998), the optimal range for the ^{220}Rn emanation from Mn-fibers is 0.3–1.0 g_{water}/g_{fiber}. Therefore, the Mn-cartridges were weighted to control their water content and were kept to a moisture range similar to that of the Mn-fibers. The water content of the Mn-cartridges mostly ranged from 0.3 to 0.7 $g_{water}/g_{cartridge}$.

2.1.2. Extraction of ^{227}Ac using Mn-fibers

At two stations (stations 32 and 38), six discrete seawater samples were collected using Niskin bottles at the same depth as the ISPs in order to validate the ^{227}Ac activities determined using Mn-cartridges. Seawater samples, which ranged from 120 to 541 L, were weighted using a Chatillon KPB-052-T Portable Bench Platform Scale. The samples were then stored in large plastic barrels and were passed by gravity through 20 g of acrylic fibers impregnated with MnO_2 (Mn-fiber) that quantitatively adsorb radium isotopes but also ^{227}Ac when the flow rate is below 1 L min^{-1}; in such conditions, Mn-fibers have been shown to extract 99 ± 1% of both Ra and Ac (Moore and Reid, 1973). ^{227}Ac analysis using RaDeCC.

Following Shaw and Moore (2002), we used Radium Delayed Coincidence Counters (RaDeCC, Scientific Computer Instruments, USA), which were primarily designed to determine ^{223}Ra and ^{224}Ra in seawater samples (Giffin et al., 1963; Moore, 2008; Moore and Arnold, 1996). Dissolved ^{227}Ac activities were determined by measuring the ^{219}Rn activities that are in secular equilibrium with ^{223}Ra and ^{227}Ac. Mn-cartridges (and Mn-fibers) were analyzed at least three months after sampling to allow ^{219}Rn, ^{223}Ra, and ^{227}Ac to equilibrate. The partially dried Mn-cartridges (and Mn-fibers) were placed in plastic cartridge (or fiber) holders in a closed helium circulation loop. Cartridges holders used for the analysis are smaller than the ones used for sampling. These small cartridges holders are designed for 4″ cartridges but we use 3″ cartridges raise with PVC pieces and are 169 mm high with a diameter of 133 mm. Helium was allowed to circulate over the Mn-cartridges (and Mn-fibers) and carried the ^{219}Rn to the scintillation cell coated with ZnS, where alpha particles produced by the ^{219}Rn decay into ^{215}Po are detected. A delayed coincidence system developed by Giffin et al. (1963) and then adapted by Moore and Arnold (1996) allowed us to discriminate the signal associated with ^{219}Rn from that of other Rn isotopes (^{220}Rn and ^{222}Rn) that are not associated with ^{227}Ac. Correction for chance coincidence counts was performed (Garcia-Solsona et al., 2008; Moore and Arnold, 1996).

The measurement of the Mn-cartridges using RaDeCC was carried out for at least 13 h and up to 24 h with the aim of increasing counting statistics. This could be achieved because of the very low background levels of the RaDeCC system (see below). Note that the background may increase due to decay products (accumulation of Rn and its daughter) remaining in the counting cells. In addition, Mn–cartridges lost up to 4.36 g of water during long counting sessions with a mean of 34 mg of water per hour (this study), which may also result in the accumulation of moisture within the detector. No effect of the moisture (between 30% and 70%) has been observed along counting or between repeated

measurements with different moisture content. In order to avert these latter issues, the scintillation cells were flushed for at least 4 h between samples to flush the system of these residual isotopes and to eventually dry the cell. We chose to conduct the analyses on only two RaDeCC systems in order to reduce the variability that may result from the use of multiple counting systems. Mn cartridges are known to extract radium isotopes, thorium isotopes but also ^{231}Pa. Therefore, a simple decay correction for ^{227}Ac activities (as usually done) is not appropriate since ^{227}Ac will also grow into equilibrium with its parent ^{231}Pa (due to the 3 to 4 year lag between sampling and analysis). Despite the fact that ^{231}Pa activities have been measured on separate samples along the section (Deng et al., 2018), the extraction efficiency of ^{231}Pa on Mn-cartridges is not known. Therefore, the amount of ^{231}Pa on Mn-cartridges are not known, which prevent from precisely quantifying the ingrowth of ^{227}Ac. Assuming a ^{231}Pa extraction efficiency of 80% on Mn-cartridges, the ^{227}Ac activities would need to be lowered by 10% (± 13%, 1 SD). If no ^{231}Pa was extracted by the Mn-cartridges, ^{227}Ac activities would need to be increased by up to 7%. Therefore, in the absence of precise information on the ^{231}Pa activity on the Mn cartridges and because the correction is small, the ^{227}Ac activities were not corrected for decay/ingrowth that occurred between sampling and analysis. ^{227}Ac activities were then corrected for Mn-cartridge extraction efficiency and normalized to the seawater volume. ^{227}Ac activities are reported in dpm m^{-3}. Despite the 100% extraction efficiency of the Mn-fibers, the ^{227}Ac activities on the Mn-fiber samples were very low, due to the reduce amount of water that was collected using Niskin bottles. Each sample was counting several times, and the counts were summed up to decrease the uncertainties. The system was flushed for 5 min in between each counting and water was added if necessary to the Mn-fiber to maintain constant moisture.

3. Results and discussion

3.1. RaDeCC performances

3.1.1. Background measurements

The RaDeCC system displays very low backgrounds. We conducted several long background counts (up to 73 h; Table 1) using two sets of Mn-coated acrylic cartridges similar to those used during the GEOVIDE cruise. These long background analyses provided a precise estimation of the background for the two detectors used in this study (Table 1). For both Mn-cartridges and Mn-fibers, the chance coincidence corrected backgrounds on channel 219 (^{219}Rn) were 0.004 and 0.002 cpm (counts per minute) for detectors #1 and #2 respectively. The backgrounds reported here were of the same order of magnitude as those previously reported in the literature for Mn-fibers (Garcia-Solsona et al., 2008; Giffin et al., 1963; Moore and Arnold, 1996). The limit of detection (LOD) and limit of quantification (LOQ) were calculated as 3 and 10 times the standard deviation of these backgrounds, respectively. As far as Mn-cartridges are concerned, LOD were 0.007 and 0.006 cpm for detectors #1 and #2, respectively, while LOQ were 0.014 cpm for both detectors (Table 1).

3.1.2. Detector efficiency

The two RaDeCC systems used in this study were calibrated using Mn-cartridge standards, i.e. Mn-cartridges containing a known amount of ^{227}Ac. Mn-cartridges were prepared using radium free seawater spiked with an ^{227}Ac solution and passed through the Mn-cartridges via gravity flow. When preparing the standard Mn-cartridge, the effluent was passed several times onto the Mn-cartridge to ensure quantitative adsorption of the ^{227}Ac spike. Mn-cartridge standards were measured using small cartridge holders in a similar manner as for samples. This standard was measured by multiple laboratories over 13 months and it has proven to be stable over time (no decrease in activity as observed by Scholten et al. (2010)). The RaDeCC systems were also calibrated for Mn-fibers using a fiber standard. A decline with time has been observed on the old Mn-fiber standard previously used to calibrated for ^{219}Rn (i.e., Mn fiber impregnated with a standard solution of ^{227}Ac and prepared at Alfred Wegener Institute (AWI, Germany) and described in van Beek et al. (2010)). Therefore, the efficiency of the systems for fibers was determined from the efficiency of the ^{220}Rn channel using a Mn-fiber impregnated with a known amount of ^{228}Th following Scholten et al. (2010). The efficiency for ^{227}Ac was then determined following Moore and Cai (2013). The standards were measured under controlled conditions (room temperature and humidity) over a 9-month period.

The detector efficiencies are reported in Table 2 for both Mn-cartridges and Mn-fibers. For Mn-cartridges, the detector efficiencies for the 219 channel were 35% ± 2% and 34% ± 2%, for detectors #1 and #2 respectively. For Mn-fiber, the efficiencies show good agreement with those for Mn-cartridges (i.e., 36% ± 3% and 34% ± 4% for

Table 1
Backgrounds for ^{219}Rn of detectors #1 and #2 for both Mn-cartridges and Mn-fibers. The limit of detection (LOD) and limit of quantification (LOQ) were calculated as 3 and 10 times the standard deviation of these backgrounds, respectively.

		Detector #1	Detector #2
	Run time (min)	^{219}Rn (cpm)	^{219}Rn (cpm)
Mn-cartridges	959	0.004	0.003
	1027	0.002	0.002
	1220	0.005	0.007
	1346	0.004	0.001
	2743	0.002	0.001
	3852	0.003	0.002
	3864	0.005	0.001
	3938	0.003	0.000
	4061	0.004	0.001
	4393	0.006	0.001
	Mean	0.004	0.002
	SD (1σ)	0.001	0.001
	LD	0.007	0.006
	LQ	0.014	0.014
Mn-fibers	377	0.003	0.003
	422	0.002	0.002
	464	0.000	0.000
	876	0.000	0.001
	924	0.001	0.000
	Mean	0.001	0.001
	SD (1σ)	0.001	0.001
	LD	0.004	0.004
	LQ	0.011	0.011

Table 2
Detector efficiencies for ^{227}Ac (for both Mn-cartridges and Mn-fibers).

	Detection efficiency (Mn-cartridge)		Detection efficiency (Mn-fiber)	
	Detector #1	Detector #2	Detector #1	Detector #2
	38%	37%	37%	28%
	36%	34%	37%	37%
	33%	34%	36%	35%
	34%	34%	37%	32%
	38%	35%	35%	29%
	34%	33%	40%	32%
	35%	32%	37%	37%
	35%	31%	37%	38%
	34%	33%	29%	38%
	35%	33%	37%	34%
Mean	**35%**	**34%**	**36%**	**34%**
SD (1σ)	**2%**	**2%**	**3%**	**4%**
n	**10**	**10**	**10**	**10**

Table 3
^{227}Ac activities determined on Mn-cartridges A for each analysis of several repeated samples are reported together with the average of ^{227}Ac activities from these repeated analyses. The internal precision corresponds to the propagated standard error (SE) and relative standard error (RSE) determined following Garcia-Solsona et al. (2008). The external precision represents the calculated standard deviation (SD) and relative standard deviation (RSD) determined from repeated measurement of the same samples are reported.

										Internal precision		External precision	
Station	Longitude (°E)	Latitude (°N)	Depth (m)	Volume (L)	Runtime (min)	^{219}Rn (counts)	^{219}Rn (cpm)	^{227}Ac on Mn-cartridges (dpm)	Mean (dpm)	SE* (1σ) (dpm)	RSE* (1σ) %	SD (1σ) (dpm)	RSD (1σ) %
1	−10.036	40.333	2500	1565	1432	115	0.080	0.09	0.15	0.02	23	0.07	48
					1025	147	0.143	0.22		0.04	15		
					1002	80	0.080	0.12		0.02	20		
13	−13.888	41.383	1500	1341.5	1013	38	0.038	0.05	0.04	0.02	34	0.01	18
					1055	40	0.038	0.04		0.02	44		
			4000	1482	998	71	0.071	0.12	0.10	0.02	20	0.03	31
					1015	42	0.041	0.06		0.02	31		
					916	43	0.047	0.10		0.05	52		
			5280	647	1216	125	0.103	0.16	0.19	0.03	18	0.04	19
					949	114	0.120	0.23		0.03	15		
					1017	99	0.097	0.18		0.09	48		
21	−19.672	46.544	2700	1417	1222	66	0.054	0.06	0.05	0.02	37	0.00	8
					903	37	0.041	0.06		0.02	34		
					1228	49	0.040	0.05		0.01	31		
			3500	1482	911	74	0.081	0.14	0.14	0.03	20	0.00	1
					1007	84	0.083	0.14		0.03	19		
26	−22.603	50.278	2023	1423	962	37	0.038	0.06	0.06	0.02	26	0.00	3
					1070	50	0.047	0.06		0.02	29		
			2843	680	1281	40	0.031	0.06	0.06	0.02	25	0.00	8
					886	31	0.035	0.05		0.02	34		
					1143	43	0.038	0.06		0.02	25		
			3563	1351	1053	58	0.055	0.08	0.09	0.02	24	0.01	7
					955	51	0.053	0.09		0.02	25		
					989	53	0.054	0.09		0.05	54		
			3868	581	1130	62	0.055	0.09	0.12	0.02	23	0.04	32
					1027	93	0.091	0.14		0.03	18		
32	−26.710	55.506	800	1378	1086	43	0.040	0.02	0.03	0.02	68	0.00	14
					1035	29	0.028	0.03		0.01	49		
			2267	1334	976	27	0.028	0.03	0.03	0.02	56	0.01	28
					967	24	0.025	0.04		0.01	36		
			2854	1265	1041	40	0.038	0.07	0.05	0.02	27	0.01	28
					1038	35	0.034	0.05		0.02	31		
					967	18	0.019	0.04		0.01	38		
					1089	34	0.031	0.04		0.02	42		
38	−31.267	58.843	1316	1166	1002	47	0.047	0.03	0.04	0.02	61	0.00	12
					1003	51	0.051	0.04		0.02	46		
					1179	34	0.029	0.04		0.02	35		
44	−38.954	59.623	2560	149	1036	71	0.069	0.10	0.11	0.03	24	0.01	11
					1292	101	0.078	0.12		0.03	20		
64	−46.083	59.068	400	1068	1014	68	0.067	0.07	0.06	0.02	31	0.02	26
					962	55	0.057	0.05		0.02	44		
			1716	1169	1027	34	0.033	0.05	0.05	0.02	33	0.00	3
					990	40	0.040	0.05		0.02	39		
69	−48.093	55.841	460	952	1032	44	0.043	0.06	0.05	0.02	53	0.02	40
					1074	49	0.046	0.03		0.02	54		
			2463	418	1147	58	0.051	0.07	0.08	0.02	24	0.01	8
					962	45	0.047	0.08		0.02	26		
			3616	738	1393	48	0.034	0.05	0.04	0.02	30	0.01	19
					1038	23	0.022	0.03		0.01	40		
					995	30	0.030	0.04		0.01	35		
								Weighted average			34%	0.02	19%
								Standard Deviation			13%		13%

detectors #1 and #2, respectively). These efficiencies for the Mn-cartridges and Mn-fibers are in good agreement with those reported by Henderson et al., (2013) (30% to 38% and 28% to 47%, respectively).

3.1.3. Precision

The internal precision associated with the RaDeCC measurement is usually estimated through uncertainty propagation calculations as reported by (Garcia-Solsona et al., 2008). Here, the repeatability (i.e. external precision) was assessed by measuring a total of twenty (out of seventy-three) individual Mn-cartridge samples (A Mn-cartridges only) two, three, or four times (eleven duplicates, eight triplicates and one quadruplicate, yielding to a total of fifty measurements; Table 3). Standard deviations of these replicates are < 0.09 dpm (1 SD) while the relative standard deviations (1 RSD) range between 1% and 48% (Table 3), with a weighted mean value of 19% (weight of 2 for duplicates, 3 for triplicates and 4 for quadruplicates). The Fig. 1 shows that there is no clear relationship between the RSD and the ^{227}Ac activities of the Mn-cartridges notably that the repeatability does not improve with increasing ^{227}Ac activity. As a comparison, the uncertainty calculated following Garcia-Solsona et al., (2008) is 34 ± 13% (1 SD; n = 50; Table 3, for A Mn-cartridges). Forty-one measurements out of the fifty ones constituting this repeatability study have an internal precision estimated by the counting statistic propagation method reported by Garcia-Solsona et al. (2008) larger than the mean

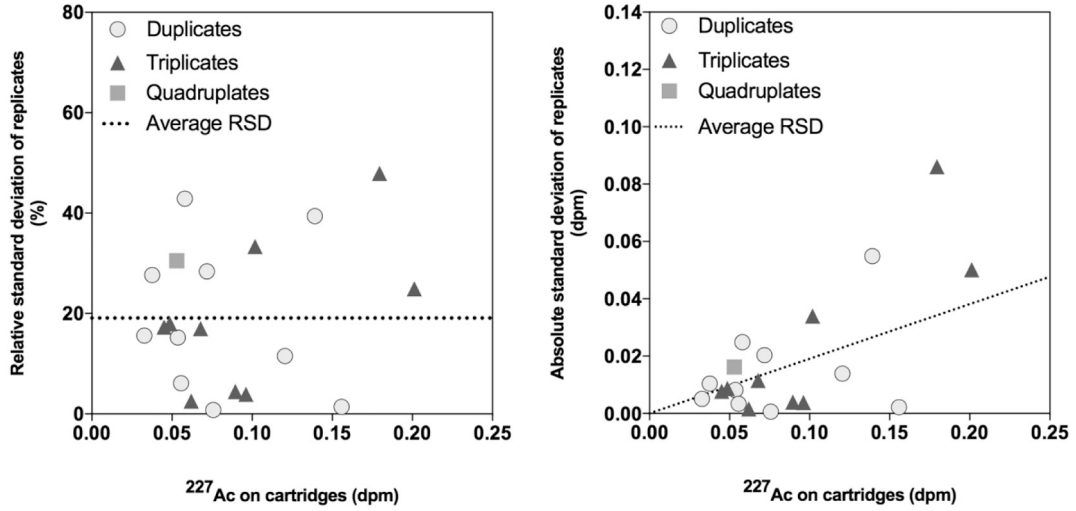

Fig. 1. Repeatability determined from replicate analyses of GEOVIDE Mn-cartridge samples expressed as the relative (left) and absolute (right) standard deviation of each replicate, versus the ^{227}Ac activities on Mn-cartridges. The weighted average (weight of 2 for duplicates, 3 for triplicates and 4 for quadruplicates) value of relative standard deviations calculated for each individual replicate is shown as dotted lines on both plots.

repeatability of 19 ± 13%. The RSD is lower (11%) for activities on Mn-cartridges from 0.06 to 0.08 cpm while for activities from 0.02 to 0.06 cpm and from 0.08 to 0.20 cpm, the RSD are 20% and 21%, respectively. The internal precision estimated by the counting statistic propagation decrease with increasing activities on the Mn-cartridges. This suggests that these uncertainty propagation calculations (Garcia-Solsona et al., 2008) may overestimate the real measurement uncertainties. This may be caused by the fact that these propagation calculations assume several hypotheses like the independence of the different variables that may not be verified. In any case, precision estimation from replicate analyses is always preferable to the error propagation calculations. Therefore, the average external precision reported above (19%, 1 SD, n = 20) is considered as the best choice for the measurement uncertainty for all the ^{227}Ac activities reported in this study.

3.2. Mn-cartridge extraction efficiencies

3.2.1. Mn-cartridges in series

The extraction efficiency for dissolved ^{227}Ac onto the Mn-cartridges was determined for each sample by measuring the ^{227}Ac activity on two Mn-cartridges mounted in series on the in situ pumps as was done in the past for other radionuclides extracted from seawater samples in a similar manner (Baskaran et al., 1993; Livingston and Cochran, 1987; Mann and Casso, 1984; van der Loeff and Moore, 1999). The extraction efficiency is determined as follows:

$$E = 1 - \frac{^{227}Ac_{Cart\ B}}{^{227}Ac_{Cart\ A}} \quad (1)$$

Where E is the dissolved ^{227}Ac extraction efficiency of the Mn-cartridges, $^{227}Ac_{cartA}$ and $^{227}Ac_{cartB}$ are the ^{227}Ac activities on the first and second Mn-cartridges placed in series, respectively. With this approach, E is assumed to be equal for both Mn-cartridges.

Among the thirty-six paired cartridges analyzed in this study, the ^{227}Ac activities on B Mn-cartridges were found to be below the limit of quantification for fifteen samples, which prevented us from estimating the extraction efficiencies for these samples (Fig. 2). One could argue that this could be due to higher than average extraction efficiencies on A cartridges combined with average or below average extraction efficiencies on B cartridges. In such a case, excluding these samples would bias our mean extraction efficiency estimation. However, the activities measured on A Mn-cartridge of most of these fifteen samples (13 out of 15) were also low. Therefore, this rules out the above mention caveat,

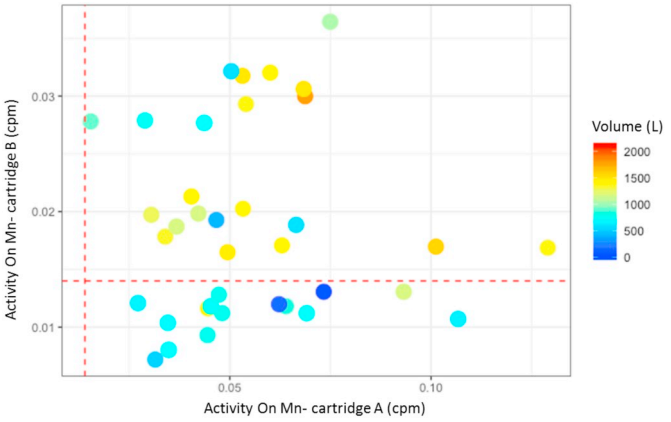

Fig. 2. ^{227}Ac activities on Mn-cartridges A vs B in. The colour scale represents the volume (V) in L. The red dashed line represents the limit of quantification (LOQ). Below this line the samples were not use to estimate the extraction efficiency. (For interpretation of the references to colour in this figure legend, the reader is referred to the web version of this article.)

and shows that these low activities on cartridges B rather reflect the combination of relatively small seawater volumes (shown in Fig. 2) and low seawater ^{227}Ac activities. Only two samples display large ^{227}Ac activities on A Mn-cartridges, suggesting that the ^{227}Ac extraction efficiency onto the Mn-cartridges is higher on the A Mn-cartridges compared with the B Mn-cartridges. Excluding these data from the mean extraction efficiency estimation does introduce a negative bias. Unfortunately we have no choice but to exclude them as B cartridge measurement is unreliable because below detection limit. However, this involves only 2 data points compared to 21 used for our estimation, thus, the negative bias is likely negligible.

Among the remaining twenty-one samples, nine samples were chosen arbitrarily for repeatability estimation (Mn-cartridge B count rates above LOQ; Table 4). Repeated analyses were thus conducted in these samples, by analyzing both Mn-cartridges A and B, in order to better constrain the extraction efficiency. The obtained extraction efficiency for all Mn-cartridges ranged from 31% to 78%, with a mean value of 47 ± 12% (1 SD, n = 21). This mean value was obtained calculating a weighted average by multiplying by one samples analyzed once, by two samples analyzed twice, by three samples analyzed three times and by four samples analyzed four times. Other estimations done

Table 4
Extraction efficiencies calculated with Mn-cartridges A and B.

Station	Longitude	Latitude	Depth	Volume	Replicates	Cartridge A				Cartridge B							
						Runtime	^{219}Rn	^{219}Rn	^{227}Ac on Mn-cartridge A	Runtime	^{219}Rn	^{219}Rn	^{227}Ac on Mn-cartridge B	Extraction efficiency	Replicates Mean	Replicates SD (1σ)	Replicates RSD (1σ)
	(°E)	(°N)	(m)	(L)		(min)	(counts)	(cpm)	(dpm)	(min)	(counts)	(cpm)	(dpm)	%	%	%	%
1	−10.036	40.333	2000	1781		800	55	0.07	0.114	800	24	0.030	0.069	40			
1	−10.036	40.333	2500	1565	a	1432	115	0.08	0.089	1432	22	0.015	0.024	73	78	7	9
					b	1025	147	0.14	0.224	1025	18	0.018	0.031	86			
					c	1002	80	0.08	0.123	1002	18	0.018	0.032	74			
1	−10.036	40.333	3450	1353		1008	130	0.13	0.086	1008	17	0.017	0.052	40			
13	−13.888	41.383	3000	1396		999	60	0.06	0.122	999	32	0.032	0.071	42			
13	−13.888	41.383	4000	1482	a	998	71	0.07	0.123	998	34	0.034	0.070	43	35	8	23
					b	1015	42	0.04	0.063	1015	30	0.030	0.046	27			
					c	916	43	0.05	0.102	916	29	0.032	0.067	34			
13	−13.888	41.383	4850	694		939	41	0.04	0.094	939	26	0.028	0.048	49			
13	−13.888	41.383	5280	647	a	1216	125	0.10	0.164	1216	12	BDL	BDL	n.d.			
					b	949	114	0.12	0.233	949	9	BDL	BDL	n.d.			
					c	1017	99	0.10	0.181	1017	13	BDL	BDL	n.d.			
21	−19.672	46.544	2700	1417	a	1222	66	0.05	0.056	1222	25	0.020	0.030	46	35	15	44
					b	903	37	0.04	0.058	903	20	0.022	0.044	24			
					c	1228	49	0.04	0.050	1228	15	BDL	BDL	n.d.			
21	−19.672	46.544	3500	1482	a	911	74	0.08	0.142	911	29	0.032	0.071	50	42	12	28
					b	1007	84	0.08	0.139	1007	39	0.039	0.092	34			
21	−19.672	46.544	3944	717		1016	46	0.05	0.056	1016	12	BDL	BDL	n.d.			
21	−19.672	46.544	4444	719		1071	74	0.07	0.102	1071	12	BDL	BDL	n.d.			
26	−22.603	50.278	2843	680	a	1281	40	0.03	0.059	1281	12	BDL	BDL	n.d.			
					b	1143	43	0.04	0.062	1143	21	0.018	0.026	58			
26	−22.603	50.278	3563	1351	a	1053	58	0.06	0.080	1053	35	0.033	0.055	31	38	2	6
					b	955	51	0.05	0.088	955	31	0.032	0.059	34			
					c	989	53	0.05	0.092	989	22	0.022	0.046	50			
26	−22.603	50.278	3868	581	a	1130	62	0.05	0.091	1130	16	0.014	0.030	67			
					b	1027	93	0.09	0.144	1146	15	BDL	BDL	n.d.			
26	−22.603	50.278	4126	1031.5		961	72	0.07	0.136	961	35	0.036	0.078	43			
32	−26.710	55.506	1481	1442.5		971	48	0.05	0.069	971	16	0.016	0.021	70			
32	−26.710	55.506	2267	1333.5	a	976	27	0.03	0.027	976	14	0.014	0.020	26	31	8	24
					b	967	24	0.02	0.041	1279	29	0.023	0.026	37			
32	−26.710	55.506	2854	1265	a	1041	40	0.04	0.067	1041	17	0.016	0.023	65	38	39	101
					b	1038	35	0.03	0.053	1038	24	0.023	0.047	11			
					c	1089	34	0.03	0.041	1089	12	BDL	BDL	n.d.			
32	−26.710	55.506	3050	89		995	73	0.07	0.009	995	13	BDL	BDL	n.d.			
32	−26.710	55.506	3170	771		894	43	0.05	0.062	892	10	BDL	BDL	n.d.			
38	−31.267	58.843	643	770		1015	48	0.05	0.042	1015	13	BDL	BDL	n.d.			
38	−31.267	58.843	840	1389		937	59	0.06	0.050	937	16	0.017	0.021	59			
38	−31.267	58.843	1087	697		1120	39	0.03	0.025	1120	9	BDL	BDL	n.d.			
38	−31.267	58.843	1235	656		993	27	0.03	0.045	993	12	BDL	BDL	n.d.			
38	−31.267	58.843	1316	1166	a	1002	47	0.05	0.034	1002	14	BDL	BDL	n.d.	32	18	58
					b	1003	51	0.05	0.042	1004	21	0.021	0.031	26			
					c	1179	34	0.03	0.043	1179	29	0.025	0.027	37			
44	−38.954	59.623	1136	901		971	15	0.02	0.023	971	27	0.028	0.005	79			
44	−38.954	59.623	2746	1374		938	50	0.05	0.038	938	19	0.020	0.018	54			
44	−38.954	59.623	2880	838		1016	65	0.06	0.064	1016	12	BDL	BDL	n.d.			
64	−46.083	59.068	1716	1169	a	1027	34	0.03	0.052	1027	27	0.026	0.034	34			
					b	990	40	0.04	0.050	990	11	BDL	BDL	n.d.			
64	−46.083	59.068	2060	523		1112	35	0.03	0.051	1112	8	BDL	BDL	n.d.			

(*continued on next page*)

Table 4 (*continued*)

Station	Longitude	Latitude	Depth	Volume	Replicates	Cartridge A				Cartridge B				Extraction efficiency	Replicates Mean	Replicates SD (1σ)	Replicates RSD (1σ)
						Runtime	^{219}Rn	^{219}Rn	^{227}Ac on Mn-cartridge A	Runtime	^{219}Rn	^{219}Rn	^{227}Ac on Mn-cartridge B				
	(°E)	(°N)	(m)	(L)		(min)	(counts)	(cpm)	(dpm)	(min)	(counts)	(cpm)	(dpm)	%	%	%	%
64	−46.083	59.068	2313	1365		1032	46	0.04	0.053	1032	12	BDL	BDL	n.d.			
64	−46.083	59.068	2443	576		933	47	0.05	0.076	933	30	0.032	0.033	57			
69	−48.093	55.841	2463	418	a	1147	58	0.05	0.073	1147	18	0.016	0.018	75	64	17	26
					b	962	45	0.05	0.081	962	22	0.023	0.039	52			
69	−48.093	55.841	2953	776		967	43	0.04	0.050	967	9	BDL	BDL	n.d.			
69	−48.093	55.841	3440	1169		1148	107	0.09	0.123	1148	15	BDL	BDL	n.d.			
69	−48.093	55.841	3616	738	a	1393	48	0.03	0.050	1393	36	0.026	0.034	31	35	10	29
					b	1038	23	0.02	0.034	1038	36	0.035	0.028	17			
					c	995	30	0.03	0.042	995	23	0.023	0.018	56			
													Weighted average		47	12	

by excluding either samples displaying relatively small seawater volumes (i.e. below 1000 L), or samples displaying low ^{227}Ac activities yield to the same values within errors. This extraction efficiency (E) of 47% was applied to all samples (including samples collected using single Mn-cartridges and samples collected using Mn-cartridges in series). Finally, the ^{227}Ac activities of the seawater samples, A_{227Ac}, were estimated as follows:

$$A_{^{227}Ac} = \frac{^{227}Ac_{Cart\ A}}{E} \quad (2)$$

The extraction efficiency of 47 ± 12% is lower than those reported by previous studies. In a study conducted in the Pacific Ocean, Kipp et al. (2015) assumed an ^{227}Ac extraction efficiency for Mn-cartridges of 70%. However, this value was not determined by analyzing ^{227}Ac directly in the Mn-cartridges. In this latter study, the extraction efficiencies have been determined for Ra and Th isotopes. A mean value was thus determined from these Ra and Th extraction efficiencies (i.e. 70%) and was actually considered to be representative of ^{227}Ac Mn-cartridge extraction efficiency. Geibert and Vöge (2008) and Geibert et al. (2002) reported extraction efficiencies for ^{227}Ac of 77 ± 13% (n = 14) and 69 ± 11% (n = 31), while Kemnitz (2018) and Hammond et al., (pers. comm.) reported mean extraction efficiencies for ^{227}Ac of 54% and 65%, respectively (Table 5). A significant variability in the ^{227}Ac extraction efficiencies is thus observed. Such variability may be due to the composition of the Mn-cartridges (acrylic vs polypropylene) or to the size of the Mn-cartridges used in the different studies or to a combination of the two (Table 5). Leaks may also reduce the extraction efficiency, in case the sealing between the cartridge holder and the Mn-cartridge is not optimal; such a problem cannot be completely excluded in the present study, since the relatively small Mn-cartridges that we used were placed into large cartridge holders. Geibert and Vöge (2008) used the largest Mn-cartridges (25 cm long polypropylene cartridges) and obtained relatively high extraction efficiencies. (Kemnitz, 2018) used smaller Mn-cartridges (12.7 cm long acrylic Mn-cartridges) and the extraction efficiency was significantly reduced compared to Hammond et al., (pers. comm.) who used the same length of Mn-cartridges but used cellulose instead of acrylic. The Mn-cartridges used in the present studies were even shorter (7.7 cm long acrylic cartridges) and the extraction efficiency is further reduced. Both the size and the formulation of the Mn-cartridge may thus impact the yield of ^{227}Ac extraction. Note that we impregnated the Mn-cartridges using a continuous flow of $KMnO_4$ through the cartridge (see section 2.1.1.). This step does not seem to improve significantly the extraction efficiency.

In a parallel study, ^{226}Ra activities were measured in seawater samples collected during the GEOVIDE cruise at the same depth, using Mn-fibers and radon emanation technique (Le Roy et al., 2018). Several Mn-cartridges were also analyzed for ^{226}Ra by gamma spectrometry (same samples as for ^{227}Ac, unpublished data). These data allowed us to estimate the Mn-cartridge extraction efficiencies for ^{226}Ra in a similar manner as described above. The extraction efficiencies for ^{226}Ra were found on average to be 60 ± 16% (1 SD, n = 15). The ^{226}Ra extraction efficiency thus obtained is in good agreement with the extraction efficiency of ^{226}Ra on acrylic Mn-cartridges of 54% reported by (Henderson et al., 2013).

The ^{226}Ra extraction efficiency of the Mn-cartridges is thus significantly higher than the ^{227}Ac extraction efficiency estimated in the same Mn-cartridges. This result shows that assuming the same extraction efficiency between Ra and Ac could lead to significant biases. The systematic determination of the ^{227}Ac extraction efficiency seems therefore required. Finally, note that there were no significant correlations between efficiency and other parameters such as volume, flow rate, station, water depth, activity on the A Mn-cartridge or the final activity. The extraction efficiency determined in this study will thus be applied to all the samples collected along the GEOVIDE section to provide an entire section of dissolved ^{227}Ac activities.

Table 5
Comparison of the extraction efficiencies for ^{227}Ac on Mn-cartridges determined by different studies. The analytical method used, the composition and the size of the Mn-cartridges are also reported.

Reference	Mean	SD	Range			n	Analytical method	Formulation	size	Method
This study	47%	12%	31%	–	78%	9	Delayed coincidence counting	Acrylic	7.7	2 Mn-cartridges in serie
Kemnitz (2018)	54%	6%					Delayed coincidence counting	Acrylic	12.7	2 Mn-cartridges in serie
Hammond et al. (Pers. Comm.)	65%						Delayed coincidence counting	Cellulose	12.7	2 Mn-cartridges in serie
Geibert et al. (2002)	69%	11%	45%	–	90%	31	Alpha spectrometry	Polypropylene	25	2 Mn-cartridges in serie
Geibert and Vöge (2008)	77%	13%	41%	–	95%	14	Alpha spectrometry	Polypropylene	25	2 Mn-cartridges in serie
Kipp et al. (2015)	70%						Delayed coincidence counting	Cellulose	12.7	Mean between Ra and Th extraction efficiency

3.2.2. *^{227}Ac determined from Mn-cartridges vs ^{227}Ac determined from Mn-fibers*

Six discrete seawater samples were collected and were passed by gravity through Mn-fibers on board. Because Mn-fibers quantitatively adsorb ^{227}Ac (Reid et al., 1979), this allowed us to validate the ^{227}Ac activities determined from the Mn-cartridges. Note, however, that although Mn-fibers have the advantage of adsorbing 100% of ^{227}Ac, the collection of reduced volumes of seawater (120 to 541 L) with Niskin bottles yields to low activities on the Mn-fibers, and the associated uncertainties, therefore, are relatively high. Consequently, in the present paper, we did not estimate the extraction efficiency of the Mn-cartridges by comparing the ^{227}Ac activities on the Mn-Fibers and those on the Mn-cartridges. Here, we use the ^{227}Ac activities determined using Mn-fiber as a comparison.

Results are shown in Table 6. Fig. 3 shows the seawater ^{227}Ac activities determined from Mn-cartridges (corrected for the extraction efficiency) versus the seawater ^{227}Ac activities measured from the Mn-fibers. The 1:1 line is also plotted on Fig. 3. Although the two deepest samples (station 32–3051 m and 3171 m depth) are slightly outside of the 1:1 line, possibly due to lower volume (only 89 L ont Mn-cartridge) at 3051 m. The ^{227}Ac activities determined with the two methods are in relatively good agreement with each other. Overall, this Mn-cartridge vs Mn-fiber comparison gives confidence to the extraction efficiency determined here (47 ± 12%).

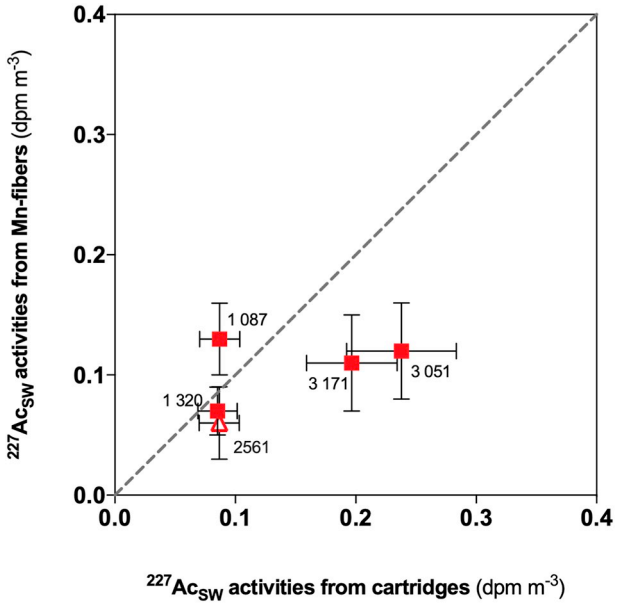

Fig. 3. Comparison of the seawater ^{227}Ac activities determined from the measurement of Mn-fibers (water sampled using Niskin bottles) and of Mn-cartridges (deployed on in situ pumps). Labels indicate the depths of the samples. One of these Mn-fibers (triangle) has no matching depth Mn-cartridge. For this sample, a mean of the ^{227}Ac activities from Mn-cartridges located below and under the Mn-fiber sample is used here. The grey line represents the 1:1 line.

3.3. *Comparison with historical data*

There are a limited number of studies that have reported ^{227}Ac activities in the open ocean to date (Geibert et al., 2008, 2002; Kipp et al., 2015; Koch-Larrouy et al., 2015; Nozaki, 1984). Fig. 4 includes these ^{227}Ac profiles determined in the open ocean in different oceanic basins together with station 32 and 38 from GEOVIDE cruise (this study). Above 2000 m, ^{227}Ac activities from the GEOVIDE cruise in the North Atlantic are within the same range of those determined in the Arctic Ocean and the Pacific Ocean. Below 2000 m, ^{227}Ac activities from the GEOVIDE cruise are lower than in other basins except for the Arctic Ocean. The ^{227}Ac activities from North Atlantic (GA03; Kipp et al., 2015) were measured in samples collected in a hydrothermal plume over the mid-Atlantic ridge in the Atlantic Ocean, which explain the higher ^{227}Ac compare to our study (GEOVIDE). The low ^{231}Pa activities along the GEOVIDE section, compare to other basins, are due to ventilated overflow waters in the North Atlantic, particularly in the Labrador and Irminger Seas (Deng et al., 2018). The low ^{231}Pa activities

Table 6
Comparison between ^{227}Ac activities determined from Mn-fibers and from Mn-cartridges A (uncorrected for extraction efficiency). The dissolved ^{227}Ac activities in seawater estimated using Mn-cartridges (corrected for extraction efficiency) are also reported. The standard deviation (SD) is determined from repeated measurement of the same samples as described in section 3.1.3.

Station	Depth	Mn-fiber					Mn-cartridges					
		Runtime	^{219}Rn	^{219}Rn	^{227}Ac	SD (1σ)	Runtime	^{219}Rn	^{219}Rn	^{227}Ac on Mn-cartridge A	^{227}Ac in SW	SD (1σ)
	(m)	(min)	(counts)	(cpm)	(dpm m^{-3})		(min)	(counts)	(cpm)	(dpm m^{-3})		
32	2267						972	33	0.034	0.03	0.072	0.013
32	2561	4153	29	0.007	0.058	0.028					0.078	0.014
32	2854						1089	34	0.031	0.04	0.084	0.015
32	3051	4153	47	0.011	0.118	0.037	995	73	0.073	0.10	0.212	0.039
32	3171	4153	37	0.009	0.108	0.037	894	43	0.048	0.08	0.175	0.032
32	3217	4153	61	0.015	0.184	0.049						
38	1087	4090	79	0.019	0.126	0.031	1120	39	0.035	0.04	0.078	0.014
38	1320	4060	142	0.035	0.067	0.017	1061	44	0.042	0.03	0.074	0.014

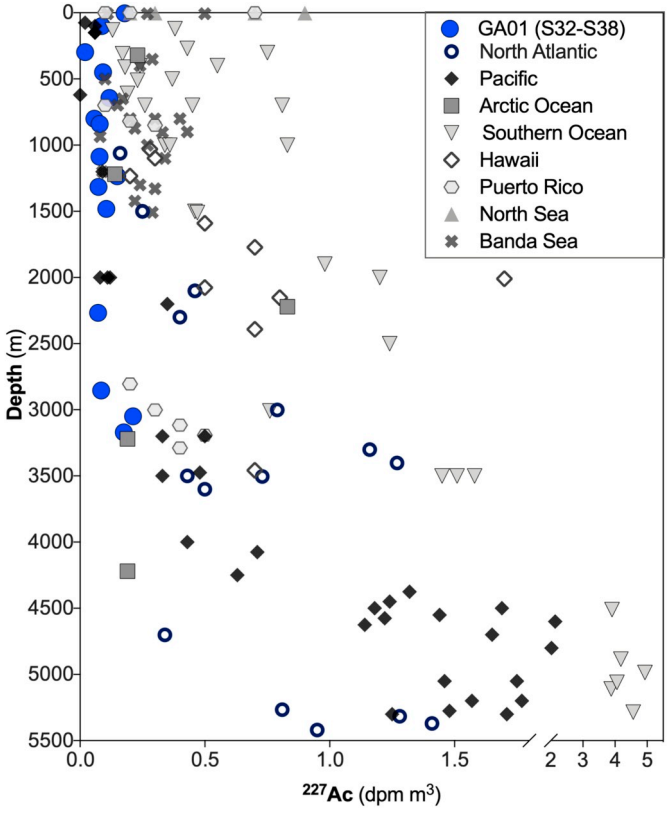

Fig. 4. ^{227}Ac activities versus depth published to date in the water columns of different oceanic basins (Geibert et al., 2008, 2002; Kipp et al., 2015; Koch-Larrouy et al., 2015; Nozaki, 1984), together with the ^{227}Ac activities determined at station 32 and 38 along the GEOVIDE section.

in the North Atlantic lead to a small production of ^{227}Ac which explain the relatively low ^{227}Ac activities compare to the Southern Ocean or in deep water of the Pacific Ocean.

3.4. Seawater ^{227}Ac vertical profiles and comparison with ^{231}Pa

In the aim of further validating the protocol, vertical profiles of ^{227}Ac—determined from Mn-cartridges and from Mn-fibers—are compared to the vertical profiles of ^{231}Pa at stations 32 and 38 (Fig. 5; ^{231}Pa

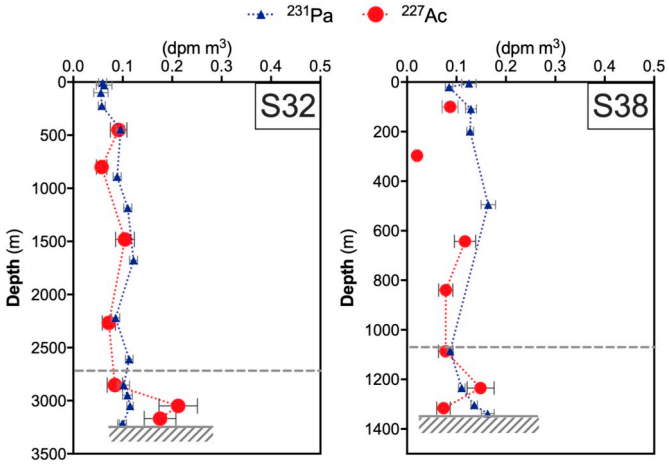

Fig. 5. Vertical profiles of dissolved ^{227}Ac (from Mn-cartidges and Mn-fibers) determined at stations 32 and 38 along the GEOVIDE section (GEOTRACES GA01) in the Iceland Basin. For comparison, the dissolved ^{231}Pa activities vertical profiles are also reported (black dots, data from Deng et al., 2018).

data from Deng et al., 2018). ^{231}Pa and ^{227}Ac have different chemical behavior in the water column. ^{231}Pa adsorbs onto particle surfaces and is thus scavenged by settling particles. In contrast, ^{227}Ac is less reactive and is supposed to remain in the dissolved phase. In the first 2000 m, ^{227}Ac is produced by the decay of the remaining ^{231}Pa in the water column. Therefore, ^{227}Ac and ^{231}Pa activities are expected to be at secular equilibrium in the upper ~2000 m, away from external sources of ^{227}Ac. ^{227}Ac and ^{231}Pa activities show a good agreement within error bars above 2000 m where ^{227}Ac and ^{231}Pa are expected to be in secular equilibrium because ^{227}Ac is produced in the water column from the ^{231}Pa decay (Nozaki et al., 1990). This is an additional validation of the overall protocol described here. The error bars reported here for the dissolved ^{227}Ac activities (repeatability experiment, 19% 1 SD) suggest the validation of the overall protocol and its accuracy, including its trueness (absence of bias, cf. good agreement with ^{231}Pa) and its precision (the internal precision of 19%, cf. error bars on the plot).

At station 38, the ^{231}Pa activities increase close to the bottom. The ^{227}Ac activities do not seem to follow such a pattern. The ^{227}Ac activities are thus significantly below ^{231}Pa activities close to bottom at 1300 m. This is an unexpected feature, as one may expect that ^{227}Ac and ^{231}Pa are at secular equilibrium over such water columns, or in excess close to bottom. This pattern could be associated to the presence of nepheloid layers (Gourain et al., 2018). Presence of MnO_2 resuspended from the sediments may adsorb ^{227}Ac, while ^{231}Pa may be released from resuspended particles. At station 32, below 2000 m, the ^{227}Ac activities are significantly higher than the ^{231}Pa activities. These excess ^{227}Ac activities likely reflect input of unsupported ^{227}Ac from the deep-sea sediments as previously observed in other ocean basins (Geibert et al., 2002; Nozaki, 1984; Nozaki et al., 1990). The entire section of dissolved ^{227}Ac activities will be reported in a separate paper (Le Roy et al., in prep.), where it will be compared to the section of dissolved ^{231}Pa activities (Deng et al., 2018), and also to several other trace elements.

4. Conclusion

This study shows that ^{227}Ac can be measured accurately in the open ocean using Mn-cartridges mounted on in situ pumps and using the RaDeCC system. This study is the second one using Mn-cartridges to extract ^{227}Ac from seawater followed by their analysis using RaDeCC and is the first one that aims to quantify the extraction efficiencies of ^{227}Ac on Mn-cartridges using Mn-cartridges placed in series. The low background of the RaDeCC systems leads to a limit of quantification of 0.014 cpm (10 times the SD). Extraction efficiencies of ^{227}Ac from seawater using Mn-cartridges were measured to be 47 ± 12% (1 SD, n = 9) for sample sizes from 418 to 1565 L. For seawater with low ^{227}Ac activities such as in the North Atlantic, a minimum of 800 L per samples would be recommended so that significant activities on the Mn-cartridge B can be quantified, which in turn allows us to estimate the extraction efficiency. For future studies, Mn-cartridges in series should also be placed at all water depths so that the ^{227}Ac extraction efficiency can be determined for each sample.

Replicate analyses of several samples collected during the GEOVIDE cruise allowed us to estimate that the Mn-cartridge ^{227}Ac activity measurement uncertainty is 19 ± 14% (1 SD, n = 20), that is significantly more precise than what would have been calculated through error propagation following Garcia-Solsona et al., 2008; i.e., 33%). This precision is sufficient to clearly detect and quantify ^{227}Ac variations in the North Atlantic Ocean, thus opening new perspectives to better exploit ^{227}Ac/^{231}Pa ratios (or excess ^{227}Ac activities) as oceanic tracers, notably for studying deep water mixing.

The advantages of this method are the low backgrounds of the RaDeCC detectors and reduced chemical procedures compared to other techniques (Geibert and Vöge, 2008; Shaw and Moore, 2002). An additional advantage of the delay coincidence counting method is that it is possible to analyze radium and thorium isotopes at the same time.

However, extraction efficiency for radium and thorium would be different from ^{227}Ac extraction efficiency.

In the aim of further validating the protocol, two vertical profiles from the GEOVIDE cruise were reported. Above 2000 m ^{227}Ac is in equilibrium with its parent ^{231}Pa, which do validate the protocol. Below 2000 m, ^{227}Ac excesses compared to ^{231}Pa may be used to estimate sedimentary fluxes of ^{227}Ac or—as was suggested by previous studies—to study vertical mixing in the deep ocean on time scales of years to decades, especially in association with other radionuclides such as ^{228}Ra. The low ^{227}Ac activities reported along the GEOVIDE section, compare to other basins, suggest recently ventilated overflow waters in the North Atlantic. Overall, the technique is validated and offers significant advantages over previous techniques. This opens up opportunities for large sections in the future, particularly in the context of the GEOTRACES programme.

Acknowledgment

Emilie Le Roy's fellowship is co-funded by the European Union and the Région Occitanie-Pyrénées-Méditerranée (SELECT Project, European Regional Development Fund). This work was supported by the French National Research Agency (ANR-13-BS06-0014, ANR-12-PDOC-0025-01), the French National Centre for Scientific Research (CNRS-LEFE-CYBER), the LabexMER (ANR-10-LABX-19), and Ifremer. It was supported for the logistic by DT-INSU and GENAVIR. We are greatly thankful to the captain, Gilles Ferrand, and crew of the N/O Pourquoi Pas? for their help during the GEOVIDE mission, as well as to the chief scientists Géraldine Sarthou and Pascale Lherminier. We would like to give a special thanks to Pierre Branellec, Floriane Desprez de Gésincourt, Michel Hamon, Catherine Kermabon, Philippe Le Bot, Stéphane Leizour, Olivier Ménage, Fabien Pérault and Emmanuel de Saint Léger for their technical expertise and to Catherine Schmechtig for the GEOVIDE database management. We acknowledge Frédéric Planchon, Hélène Planquette, Yi Tang, Maxi Castrillejo, Nolwenn Lemaître and Catherine Jeandel for their help during ISP deployment and sampling.

References

Anderson, R.F., Bacon, M.P., Brewer, P.G., 1983. Removal of 230Th and 231Pa from the open ocean. Earth Planet. Sci. Lett. 62, 7–23. https://doi.org/10.1016/0012-821X(83)90067-5.

Baskaran, M., Murphy, D.J., Santschi, P.H., Orr, J.C., Schink, D.R., 1993. A method for rapid in situ extraction and laboratory determination of Th, Pb, and Ra isotopes from large volumes of seawater. Deep Sea Res. Part Oceanogr. Res. Pap. 40, 849–865. https://doi.org/10.1016/0967-0637(93)90075-E.

Deng, F., Henderson, G.M., Castrillejo, M., Perez, F.F., 2018. Evolution of 231Pa and 230Th in overflow waters of the North Atlantic. Biogeosci. Discuss. 2018, 1–24. https://doi.org/10.5194/bg-2018-191.

Dulaiova, H., Sims, K.W.W., Charette, M.A., Prytulak, J., Blusztajn, J.S., 2012. A new method for the determination of low-level actinium-227 in geological samples. J. Radioanal. Nucl. Chem. 296, 279–283. https://doi.org/10.1007/s10967-012-2140-0.

Garcia-Solsona, E., Garcia-Orellana, J., Masqué, P., Dulaiova, H., 2008. Uncertainties associated with 223Ra and 224Ra measurements in water via a delayed coincidence counter (RaDeCC). Mar. Chem., Meas. Radium Actinium Isot. Mar. Environ. 109, 198–219. https://doi.org/10.1016/j.marchem.2007.11.006.

Geibert, W., Vöge, I., 2008. Progress in the determination of 227Ac in sea water. Mar. Chem., Meas. Radium Actinium Isot. Mar. Environ. 109, 238–249. https://doi.org/10.1016/j.marchem.2007.07.012.

Geibert, W., Rutgers van der Loeff, M.M., Hanfland, C., Dauelsberg, H.-J., 2002. Actinium-227 as a deep-sea tracer: sources, distribution and applications. Earth Planet. Sci. Lett. 198, 147–165. https://doi.org/10.1016/S0012-821X(02)00512-5.

Geibert, W., Charette, M., Kim, G., Moore, W.S., Street, J., Young, M., Paytan, A., 2008. The release of dissolved actinium to the ocean: a global comparison of different end-members. Mar. Chem., Meas. Radium Actinium Isot. Mar. Environ. 109, 409–420. https://doi.org/10.1016/j.marchem.2007.07.005.

Giffin, C., Kaufman, A., Broecker, W., 1963. Delayed coincidence counter for the assay of actinon and thoron. J. Geophys. Res. 68, 1749–1757. https://doi.org/10.1029/JZ068i006p01749.

Gourain, A., Planquette, H., Cheize, M., Lemaitre, N., Menzel Barraqueta, J.-L., Shelley, R., Lherminier, P., Sarthou, G., 2018. Inputs and processes affecting the distribution of particulate iron in the North Atlantic along the GEOVIDE (GEOTRACES GA01) section. Biogeosci. Discuss. 2018, 1–42. https://doi.org/10.5194/bg-2018-234.

Henderson, P., Morris, P., Moore, W., Charette, M., 2013. Methodological advances for measuring low-level radium isotopes in seawater. J. Radioanal. Nucl. Chem. 296, 357–362. https://doi.org/10.1007/s10967-012-2047-9.

Joint Committee for Guides in Metrology, 2008. JCGM 200: 2012 International Vocabulary of Metrology - Basic and General Concepts and Associated Terms. (VIPM) - JCGM_200_2012.pdf).

Kemnitz, N.J., 2018. Actinium-227 as Tracer for Mixing in the Deep Northeast Pacific. University of Southern California.

Kipp, L.E., Charette, M.A., Hammond, D.E., Moore, W.S., 2015. Hydrothermal vents: a previously unrecognized source of actinium-227 to the deep ocean. Mar. Chem. 177, 583–590. https://doi.org/10.1016/j.marchem.2015.09.002. Part 4.

Koch-Larrouy, A., Atmadipoera, A., van Beek, P., Madec, G., Aucan, J., Lyard, F., Grelet, J., Souhaut, M., 2015. Estimates of tidal mixing in the Indonesian archipelago from multidisciplinary INDOMIX in-situ data. Deep Sea Res. Part Oceanogr. Res. Pap. 106, 136–153. https://doi.org/10.1016/j.dsr.2015.09.007.

Ku, T.-L., Knauss, K.G., Mathieu, G.G., 1977. Uranium in open ocean: concentration and isotopic composition. Deep Sea Res. 24, 1005–1017. https://doi.org/10.1016/0146-6291(77)90571-9.

Le Roy, E., Sanial, V., Charette, M.A., van Beek, P., Lacan, F., Jacquet, S.H.M., Henderson, P.B., Souhaut, M., García-Ibáñez, M.I., Jeandel, C., Pérez, F.F., Sarthou, G., 2018. The ^{226}Ra–Ba relationship in the North Atlantic during GEOTRACES-GA01. Biogeosciences 15, 3027–3048. https://doi.org/10.5194/bg-15-3027-2018.

Livingston, H.D., Cochran, J.K., 1987. Determination of transuranic and thorium isotopes in ocean water: in solution and in filterable particles. J. Radioanal. Nucl. Chem. 115, 299–308. https://doi.org/10.1007/BF02037445.

Mann, D.R., Casso, S.A., 1984. In situ chemisorption of radiocesium from seawater. Mar. Chem. 14, 307–318. https://doi.org/10.1016/0304-4203(84)90027-6.

Moore, W.S., 2008. Fifteen years experience in measuring 224Ra and 223Ra by delayed-coincidence counting. Mar. Chem. 109, 188–197. https://doi.org/10.1016/j.marchem.2007.06.015. Measurement of Radium and Actinium Isotopes in the marine environment.

Moore, W.S., Arnold, R., 1996. Measurement of 223Ra and 224Ra in coastal waters using a delayed coincidence counter. J. Geophys. Res. Oceans 101, 1321–1329. https://doi.org/10.1029/95JC03139.

Moore, W.S., Cai, P., 2013. Calibration of RaDeCC systems for 223Ra measurements. Mar. Chem. 156, 130–137. https://doi.org/10.1016/j.marchem.2013.03.002. Radium and Radon Tracers in Aquatic Systems.

Moore, W.S., Reid, D.F., 1973. Extraction of radium from natural waters using manganese-impregnated acrylic fibers. J. Geophys. Res. 78, 8880–8886. https://doi.org/10.1029/JC078i036p08880.

Nozaki, Y., 1984. Excess 227Ac in deep ocean water. Nature 310, 486–488. https://doi.org/10.1038/310486a0.

Nozaki, Y., 1993. Actinium-227: A steady state tracer for the Deep-Sea Basin-wide circulation and mixing studies. In: Teramoto, T. (Ed.), Elsevier Oceanography Series, Deep Ocean Circulation. Elsevier, pp. 139–156. https://doi.org/10.1016/S0422-9894(08)71323-0.

Nozaki, Y., Yamada, M., Nikaido, H., 1990. The marine geochemistry of actinium-227: evidence for its migration through sediment pore water. Geophys. Res. Lett. 17, 1933–1936. https://doi.org/10.1029/GL017i011p01933.

Nozaki, Y., Yamada, M., Nakanishi, T., Nagaya, Y., Nakamura, K., Shitashima, K., Tsubota, H., 1998. The distribution of radionuclides and some trace metals in the water columns of the Japan and Bonin trenches. Oceanol. Acta 21, 469–484. https://doi.org/10.1016/S0399-1784(98)80031-5.

Reid, D.F., Key, R.M., Schink, D.R., 1979. Radium, thorium, and actinium extraction from seawater using an improved manganese-oxide-coated fiber. Earth Planet. Sci. Lett. 43, 223–226. https://doi.org/10.1016/0012-821X(79)90205-X.

Scholten, J.C., Pham, M.K., Blinova, O., Charette, M.A., Dulaiova, H., Eriksson, M., 2010. Preparation of Mn-fiber standards for the efficiency calibration of the delayed coincidence counting system (RaDeCC). Mar. Chem. 121, 206–214. https://doi.org/10.1016/j.marchem.2010.04.009.

Shaw, T.J., Moore, W.S., 2002. Analysis of 227Ac in seawater by delayed coincidence counting. Mar. Chem. 78, 197–203. https://doi.org/10.1016/S0304-4203(02)00022-1.

Sun, Y., Torgersen, T., 1998. The effects of water content and Mn-fiber surface conditions on 224Ra measurement by 220Rn emanation. Mar. Chem. 62, 299–306. https://doi.org/10.1016/S0304-4203(98)00019-X.

van Beek, P., Souhaut, M., Reyss, J.-L., 2010. Measuring the radium quartet (228Ra, 226Ra, 224Ra, 223Ra) in seawater samples using gamma spectrometry. J. Environ. Radioact. 101, 521–529. https://doi.org/10.1016/j.jenvrad.2009.12.002.

van der Loeff, M.M.R., Moore, W.S., 1999. Determination of natural radioactive tracers. In: Grasshoff, K., Kremling, K., Ehrhardt, nfred (Eds.), Methods of Seawater Analysis. Wiley-VCH Verlag Gmb H, pp. 365–397. https://doi.org/10.1002/9783527613984.ch13.